PHYSICAL REVIEW B **93**, 214503 (2016)

Superconductivity and ferromagnetism in hole-doped $RbEuFe_4As_4$

Yi Liu,[1] Ya-Bin Liu,[1] Zhang-Tu Tang,[1] Hao Jiang,[1,*] Zhi-Cheng Wang,[1] Abduweli Ablimit,[1] Wen-He Jiao,[2] Qian Tao,[1] Chun-Mu Feng,[1] Zhu-An Xu,[1,3,4] and Guang-Han Cao[1,3,4,†]

[1]*Department of Physics, Zhejiang University, Hangzhou 310027, China*

[2]*Department of Physics, Zhejiang University of Science and Technology, Hangzhou 310023, China*

[3]*State Key Lab of Silicon Materials, Zhejiang University, Hangzhou 310027, China*

[4]*Collaborative Innovation Centre of Advanced Microstructures, Nanjing 210093, China*

(Received 18 April 2016; published 8 June 2016)

We discover a robust coexistence of superconductivity and ferromagnetism in an iron arsenide $RbEuFe_4As_4$. The new material crystallizes in an intergrowth structure of $RbFe_2As_2$ and $EuFe_2As_2$, such that the Eu sublattice turns out to be primitive instead of being body-centered in $EuFe_2As_2$. The FeAs layers, featured by asymmetric As coordinations, are hole doped due to charge homogenization. Our combined measurements of electrical transport, magnetization, and heat capacity unambiguously and consistently indicate bulk superconductivity at 36.5 K in the FeAs layers and ferromagnetism at 15 K in the Eu sublattice. Interestingly, the Eu-spin ferromagnetic ordering belongs to a rare third-order transition, according to the Ehrenfest classification of phase transitions. We also identify an additional anomaly at ∼5 K, which is possibly associated with the interplay between superconductivity and ferromagnetism.

DOI: 10.1103/PhysRevB.93.214503

I. INTRODUCTION

Doped $EuFe_2As_2$ superconductors stand out among Fe-based superconductors (FeSCs), because the Eu^{2+} local spins ($S = 7/2$) may order *ferromagnetically* in the superconducting state [1–4]. The undoped $EuFe_2As_2$ undergoes an A-type antiferromagnetic (namely, in-plane ferromagnetic while interplane antiferromagnetic) transition at 19 K in the Eu sublattice [5–7], in addition to a spin-density wave (SDW) transition at 190 K in the Fe sublattice. In the magnetically ordered state, the Eu spins align along the crystallographic [110] direction, collinear with the Fe moments [8,9]. Upon partial P-for-As substitution, which effectively induces a chemical pressure, the Fe-site SDW order is suppressed, and then superconductivity (SC) emerges at $T_{sc} \sim 26$ K [1,2,10,11]. Simultaneously, the Eu spins become ferromagnetically ordered at $T_{Curie} \sim 20$ K, accompanied by a spin reorientation towards the [001] (or c-axis) direction [2]. Similar coexistence of Fe-based SC and Eu-spin ferromagnetism (FM) was also observed and verified in several Fe-site electron-doped $EuFe_2As_2$ systems [12–16].

Nevertheless, there have been some debates on the details of the Eu-spin ordering. In Refs. [11,17], it was argued that SC coexists with Eu-spin antiferromagnetism (AFM) in the superconducting regime of $EuFe_2(As_{1-x}P_x)_2$. Later, Zapf *et al.* [18] proposed that SC coexists with a canted AFM, such that it is virtually ferromagnetic along the c axis. These authors [19] further revised the electronic phase diagram because of the discovery of a reentrant spin glass state. Recent x-ray resonant magnetic scattering [3] and neutron scattering [4] experiments, however, indicated long-range ferromagnetic orderings for Eu spins in superconducting $EuFe_2(As_{1-x}P_x)_2$ with $x = 0.15$ and 0.19, respectively. It was demonstrated that the Eu spins align exactly along the c axis, in contradiction to the spin-canting scenario. So far, this discrepancy remains unresolved. Note that the spin-tilting angle (∼20° from the c axis, as detected by Mössbauer measurements [2,20]) coincides with the direction that connects the interlayer next-nearest (NN) Eu atoms because of the body-centered Eu sublattice. To clarify whether the Eu-sublattice type is relevant to Eu spin orientations, it is desirable to study a related material system in which Eu atoms form a primitive tetragonal lattice.

Local-moment FM and spin-singlet SC are known to be mutually incompatible [21–23], which makes their coexistence (hereafter abbreviated as FM+SC) very rare [24]. The FM+SC phenomenon observed in FeSCs has been ascribed to the multiorbital character as well as the robustness of superconductivity against magnetic fields [10,25]. On one hand, the zero-temperature upper critical magnetic field, $H_{c2}(0)$, of FeSCs is typically higher than 50 T [26,27], large enough to fight the internal exchange field, which is comparable to the hyperfine field on the Eu nucleus (∼25 T) [2]. On the other hand, the Eu-spin FM can be satisfied even in the presence of SC, because the Fe-3d multiorbitals enable both superconducting pairing (dominated by the d_{yz} and d_{zx} electrons [28]) and the Ruderman-Kittel-Kasuya-Yosida (RKKY) exchange interaction between Eu local moments. The RKKY interaction can be mediated by different Fe-3d orbitals such as $d_{x^2-y^2}$ and d_{z^2} [29]. Therefore both SC and local-moment FM can be favored in FeSCs [25].

The crucial factor that leads to Eu local-moment FM should be the interlayer RKKY interaction, since the in-plane RKKY coupling remains ferromagnetic even in the parent compound $EuFe_2As_2$. The interlayer exchange coupling ($J_R^{\perp}$) is simplified to be proportional to $\cos(2k_F r)/r^3$ for a large r, where k_F is the Fermi wave vector and r denotes the distance between local moments. This means that $J_R^{\perp}$ can be changed from negative (AFM) to positive (FM) by tuning the $k_F r$ value. The AFM-to-FM transition in $EuFe_2(As_{1-x}P_x)_2$ [10] and $Eu(Fe_{1-x}Ni_x)_2As_2$ [29] is mainly due to the change in k_F (where the heavy three-dimensional hole pocket [30] seems to be involved), simply because the interlayer Eu

*Present address: School of Physics and Optoelectronics, Xiangtan University, Xiangtan 411105, China.

†ghcao@zju.edu.cn

interatomic distance ($r_\perp$) varies only slightly. Indeed, based on a first-principles calculation [31], the effective interlayer NN magnetic coupling changes from antiferromagnetic in $EuFe_2As_2$ to ferromagnetic in $EuFe_2P_2$, while the in-plane coupling remains ferromagnetic.

The above statement suggests an alternative approach to realize the AFM-to-FM transition, which may lead to an FM+SC state as well. By constructing a crystal structure in which $r_\perp$ changes significantly, the sign of $J_R^\perp$ may be altered accordingly. We previously designed a related structure, exemplified as $KLaFe_4As_4$ (1144) [32], which can be viewed as an intergrowth of KFe_2As_2 and $LaFe_2As_2$. In the Eu analog, $AkEuFe_4As_4$ (Ak denotes an alkali metal), the Eu atoms form a *primitive* tetragonal lattice, such that the lines that connect the interlayer-NN Eu atoms are exactly parallel to the c axis. Notably, the $r_\perp$ value is roughly doubled because every alternate Eu atoms are replaced by Ak along the c axis.

Very recently, we became aware of the report of $AkAeFe_4As_4$ (Ae = Ca, Sr, and Ba) superconductors, which possess the identical 1144-type structure [33]. This work inspires us to reinvestigate our target material $AkEuFe_4As_4$. Consequently, we succeeded in synthesizing a 1144 compound $RbEuFe_4As_4$. In this paper, we report the crystal structure and physical properties of this new material. We indeed observe an Eu-spin FM at 15 K, which coexists with a bulk SC at an unexpectedly high T_{sc} of 36.5 K. Remarkably, the evidence for FM+SC is very robust, compared to the previous FM+SC phenomena in doped $EuFe_2As_2$ systems [1,11,13,14]. Apart from FM+SC, additional intriguing phenomena were also observed and discussed.

II. EXPERIMENTAL METHODS

$RbEuFe_4As_4$ polycrystalline samples were prepared via a solid-state reaction method. First, FeAs, EuAs, and RbAs were prepared using the following source materials: Rb (99.75%), As (99.999%), and Eu (99.9%) pieces and Fe powder (99.998%). The presynthesized arsenides were then ball milled separately for 10 minutes in a glove box filled with pure Ar (the water and oxygen content is below 1 ppm). Second, stoichiometric mixtures (namely, Rb:Eu:Fe:As=1:1:4:4) of Fe, FeAs, EuAs, and RbAs were homogenized, pressed into pellets, and then loaded in an alumina tubelike crucible, which was sealed in a Ta tube. The Ta tube was protected in a quartz ampoule filled with Ar gas (~0.6 bar). Third, the sample-loaded ampoule was heated rapidly to 1123-1173 K in a muffle furnace. After holding for 6 hours, the sample was quenched, similar to the approach in synthesizing $AkAeFe_4As_4$ [33]. The sample's quality could be improved by repeating the solid-state reaction.

Powder x-ray diffraction (XRD) was carried out on a PANalytical x-ray diffractometer with a monochromatic Cu-$K_{\alpha 1}$ radiation. The crystal structure was refined by a Rietveld analysis using a RIETAN software [34]. The electrical transport and heat capacity measurements were conducted on a Quantum Design physical property measurement system (PPMS-9). In the resistivity measurement, a four-electrode method and the ac transport option were employed. The sample pellet was cut into a thin rectangular bar with a dimension of $2.2 \times 1.1 \times 0.5$ mm^3, on which thin gold wires were attached with silver paint. The excitation current was set to 5.18 mA. The Hall coefficient was measured by permutating the voltage and current electrodes [35], using a thin-square sample ($1.3 \times 1.3 \times 0.12$ mm^3) with four symmetric electrodes attached. The excitation current was 20 mA, and the applied magnetic field was 80 kOe. The heat capacity was measured by a thermal relaxation method using a square-shaped sample plate with a mass of 19.5 mg. The dc magnetization for a regular shape sample (in order to estimate the demagnetization factor) was measured on a Quantum Design MPMS-5 equipment. Different kinds of protocols of zero-field cooling (ZFC) and field-cooling (FC) were employed for probing the superconducting and magnetic transitions.

III. RESULTS AND DISCUSSION

A. Crystal structure

The as-prepared sample was characterized by powder XRD. The result shows that most of the reflections can be indexed using a tetragonal lattice, whose unit-cell size ($a \sim 3.89$ Å and $c \sim 13.31$ Å) is close to other 1144-type compounds [33]. The intensity of the strongest reflection of the impurity phase, which is identified to be unreacted FeAs, is only 2.5% of that of the (103) diffraction peak of the main phase, indicating the high quality of the sample. The appearance of (hkl) reflections with $h + k + l =$ odd numbers confirms that the tetragonal lattice is primitive rather than body centered.

Figure 1 shows the Rietveld refinement profile for the powder XRD data of $RbEuFe_4As_4$. The refinement yields a weighted reliable factor R_{wp} of 5.21% and a "goodness-of-fit" parameter S of 1.49, which indicate high reliability for the crystal structure refined. As shown in the inset of Fig. 1, it is indeed an intergrowth of $RbFe_2As_2$ and $EuFe_2As_2$. It can be also viewed as a modified $EuFe_2As_2$ in which every alternate Eu atoms are replaced by Rb atoms along the c axis. It is the structural modification that changes the lattice from body-centered to primitive. Additionally, the local coordination environment for Fe atoms turns out to be

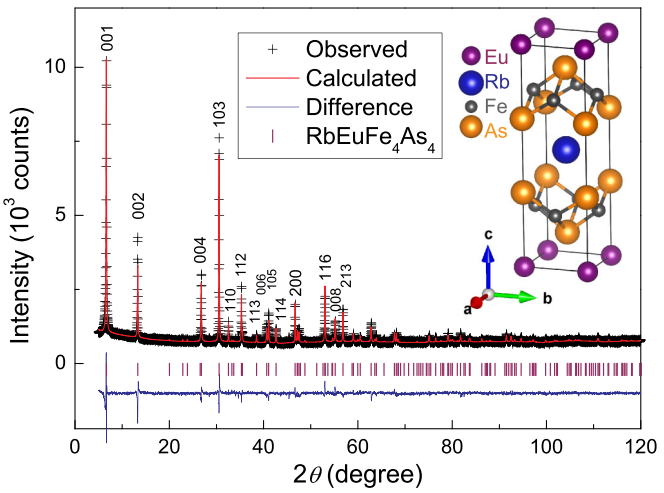

FIG. 1. Rietveld refinement profile for the powder x-ray diffraction of $RbEuFe_4As_4$ whose crystal structure is displayed in the inset. The relatively strong reflections in low diffraction angles are indexed.

TABLE I. Crystallographic data of $RbEuFe_4As_4$ at room temperature with $a = 3.8896(1)$ Å, $c = 13.3109(4)$ Å and space group $P4/mmm$ (No. 123).

Atom	Wyckoff	x	y	z	B (Å^{-2})
Eu	1a	0	0	0	2.4(2)
Rb	1d	0.5	0.5	0.5	4.2(3)
Fe	4i	0	0.5	0.2351(3)	1.6(1)
As1	2g	0	0	0.3328(4)	1.9(2)
As2	2h	0.5	0.5	0.1310(3)	2.0(2)

asymmetric. According to the refined structural parameters listed in Table I, the Fe–As bond lengths are no longer equal. Consequently, As1 (at Rb side) and As2 (at Eu side) heights from the Fe plane are remarkably different (1.300 and 1.386 Å, respectively). Meanwhile, the bond angles As1–Fe–As1 and As2–Fe–As2 are 112.50° and 109.04°, respectively. Note that the As relative heights as well as the bond angles are opposite to the result in $RbCaFe_4As_4$ [33]. This suggests that the Fe-coordination asymmetry does not interfere with the occurrence of SC, although it could influence the superconducting pairing symmetry.

Comparison of the lattice parameters of $RbEuFe_4As_4$ with those of $EuFe_2As_2$ and $RbFe_2As_2$ hints the existence of "interaction" between the two building blocks. The a axis is 0.009(2) Å smaller than the average of those of $EuFe_2As_2$ [5] and $RbFe_2As_2$ [36], meanwhile, the c axis is 0.024(5) Å smaller than half of the sum of those of $EuFe_2As_2$ and $RbFe_2As_2$. This lattice shrinkage suggests stabilization of the hybrid 1144 phase. The interaction of the two building units is also manifested by the shortening of the "$RbFe_2As_2$" block (from 7.267 to 7.052 Å) and the stretching of the "$EuFe_2As_2$" block (from 6.068 to 6.259 Å). This structural variation seems to be associated with the charge redistribution, since the Fe formal valence in $RbEuFe_4As_4$ has to be averaged to 2.25+ instead of being either 2+ in $EuFe_2As_2$ or 2.5+ in $RbFe_2As_2$. The elongation of the "$EuFe_2As_2$" block suggests weakening of the effective coupling between Eu-4f spins and Fe-3d itinerant electrons in $RbEuFe_4As_4$.

B. Electrical transport properties

Figure 2 shows electrical transport measurement results for the $RbEuFe_4As_4$ polycrystalline sample. The resistivity $\rho(T)$ exhibits a metallic behavior with a broad hump around 180 K, a common feature of hole-doped FeSCs [33,37,38]. As expected, the conduction is dominated by a hole-carrier transport, which is verified by the positive Hall coefficient (R_H) in the whole temperature range of the normal state. The R_H values appear to be extremely low (equivalent to a hole content of $n \sim 1.0$ holes/Fe using the simple formula $n = 1/(eR_H)$ for a single-band case), which indicates a multiband scenario (the electron-hole compensation effect accounts for the low R_H) [38]. A sharp superconducting transition appears at 36.5 K, and zero resistance is achieved at 36 K (note that the transition temperature in $R_H(T)$ is decreased because it was measured under an 80-kOe magnetic field). This T_{sc} value is the highest among all the doped $EuFe_2As_2$ superconductors [1,13,14,39]. Furthermore, no

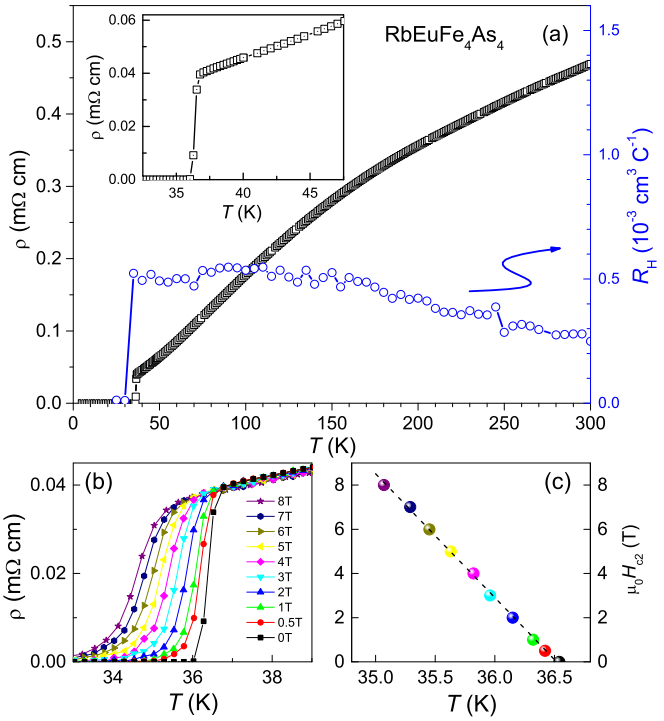

FIG. 2. (a) Temperature dependence of resistivity (left axis) and Hall coefficient (right axis) of the $RbEuFe_4As_4$ polycrystalline sample. The inset zooms in the superconducting transition under zero field. (b) The superconducting resistive transitions under increased external magnetic fields. (c) Plot of the upper critical field as a function of temperature, derived from the data shown in (b). The dashed line is the linear fit.

re-entrance superconductivity can be observed, in contrast to the case in the $EuFe_2As_2$-related ferromagnetic superconductors where nonzero resistance often re-enters the superconducting state [1,12–14].

Under external magnetic fields, the superconducting transitions shift mildly to lower temperatures, as shown in Fig. 2(b). From these data, the upper critical fields, $H_{c2}(T)$, can be obtained by defining the transition temperature $T_{sc}(H)$ at which the resistivity drops to 90% of the linearly extrapolated one (this criterion satisfies the result of heat-capacity measurement). The resulting $H_{c2}(T)$, shown in Fig. 2(c), is almost linear, in contrast with the pronounced positive curvature observed in $EuFe_2(As_{0.7}P_{0.3})_2$ [1] and $Eu(Fe_{0.88}Ir_{0.12})_2As_2$ [14]. The initial slope, $\mu_0 dH_{c2}/dT|_{T_{sc}}$, is as large as -5.6 T/K, over 4 times of that of $EuFe_2(As_{0.7}P_{0.3})_2$. Here we note that the measurement was performed on the polycrystalline sample, the $H_{c2}(T)$ data obtained actually represent some kind of average of $H_{c2}^{\|c}(T)$ and $H_{c2}^{\|ab}(T)$.

C. Magnetic properties

Figure 3 shows the dc magnetic susceptibility measured under low magnetic fields using FC and ZFC protocols, respectively. Consistent with the resistivity measurement above, a superconducting onset transition occurs at $T_{sc}^{onset} = 36.5$ K. The volume fraction of magnetic shielding, measured in a ZFC process, is almost 100% at the lowest temperature after

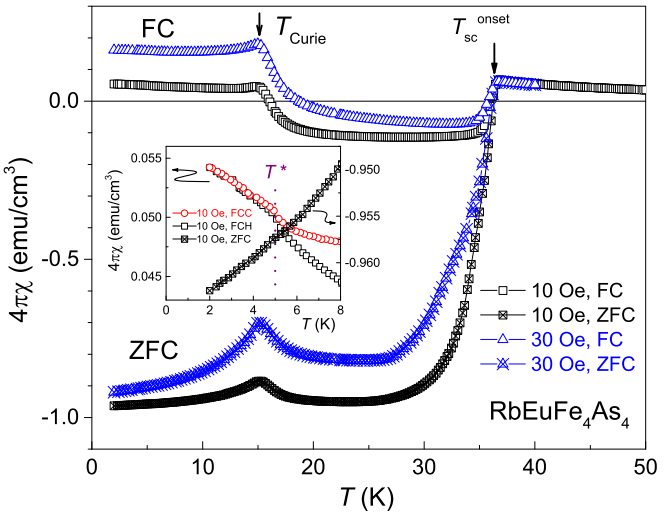

FIG. 3. Magnetic susceptibility of the $RbEuFe_4As_4$ polycrystalline sample under low magnetic fields in field-cooling (FC) and zero-field-cooling (ZFC) modes, respectively. The superconducting transition at $T_{sc}^{onset} = 36.5$ K and the magnetic transition at $T_{Curie} = 15$ K are marked by arrows, respectively. The inset magnifies low-temperature data from which a minor anomaly at $T^* = 5$ K can be distinguished. Right axis: FC data measured in cooling (FCC) and heating (FCH) processes; left axis: ZFC data.

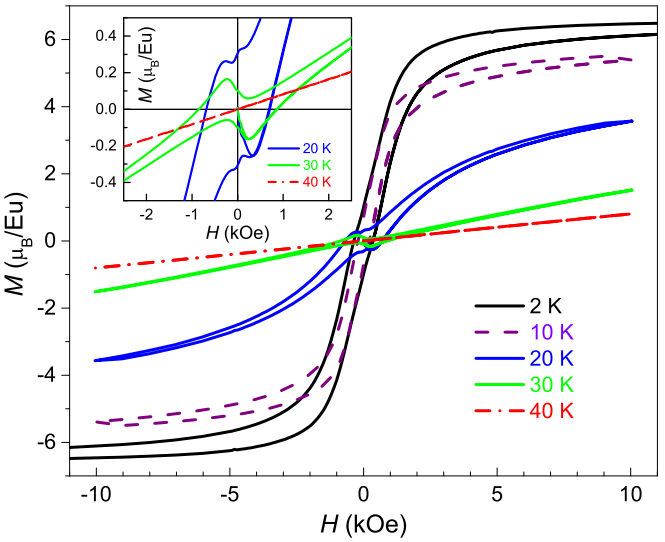

FIG. 4. Isothermal magnetization of $RbEuFe_4As_4$ at several representative temperatures. The top-left inset zooms in the data in the low-field region for $T = 20$, 30, and 40 K.

making a demagnetization correction. The volume fraction of magnetic repulsion (also called Meissner volume fraction), scaled by the drop in $4\pi\,\chi_{FC}$ in a FC process, is reduced to 16% due to flux pinning while cooling down under magnetic fields. Nevertheless, the Meissner fraction is still over six-fold higher than any impurity content (estimated to be less than 2.5% from the XRD) in the sample. Therefore, bulk superconductivity is clearly demonstrated for $RbEuFe_4As_4$. In comparison, the previous related superconductor $EuFe_2(As_{0.7}P_{0.3})_2$ shows no diamagnetism even in a ZFC process for the polycrystalline sample [1]. This facts highlight the robustness of SC in the present $RbEuFe_4As_4$ system.

Interestingly, there is an anomaly at around 15 K in the superconducting state, featured by a sign change in χ_{FC} at $H = 10$ Oe. At first sight, this behavior resembles the ac magnetic susceptibility (χ_{ac}) curve of the classical reentrant superconductor $ErRh_4B_4$ in which SC *disappears* when the Er magnetic long-range order sets in (Ref. [40]). As a matter of fact, however, χ_{ac} is equivalent to χ_{ZFC} rather than χ_{FC}. The χ_{ZFC} value of $RbEuFe_4As_4$ remains diamagnetic (in contrast with the positive χ_{ac} in $ErRh_4B_4$) in the region where χ_{FC} becomes positive, indicating SC survives at low temperatures. When the applied field is increased to 30 Oe, the χ_{FC} value is enhanced, remarkably, suggesting that it is possibly associated with ferromagnetism rather than paramagnetism. Additionally, there is a minor kink at $T^* \sim 5$ K in both FC and ZFC data, which can be seen in the magnified plot shown in the inset of Fig. 3. The bifurcation of FCC (measured in the cooling process) and FCH (measured in the heating process) can also be seen at $T > 5$ K. We will discuss the possible implications later on.

In order to further identify the 15-K transition under the superconducting state, we performed isothermal magnetization [$M(H)$] measurements. As shown in Fig. 4, the $M(H)$ data are essentially linear at $T > T_{sc}$, indicating a simple paramagnetic state. When the temperature is decreased to 30 K, which is below T_{sc} but well above 15 K, a typical superconducting loop is superposed on the paramagnetic background. At $T = 20$ K, which is close to the magnetic transition temperature, the paramagnetic component of the $M(H)$ curve takes the shape of a Brillouin function. Below 15 K, the overall $M(H)$ loop looks like that of a ferromagnet, but the magnetization curves do not merge together at fields higher than the saturation one (about 1.5 kOe). This is due to the existence of SC, which shows a flux-pinning effect as mentioned above. Note that the saturation magnetization at 2 K achieves $6.5\mu_B$/Eu, basically consistent with the expected value of $gS = 7.0\mu_B$/Eu for the Eu^{2+}-spin ferromagnetic alignment. The above results undoubtfully indicate an Eu-spin FM at $T_{Curie} = 15$ K for $RbEuFe_4As_4$, although the spin orientation is not clear. The robust ferromagnetic properties contrast with those of the previous ferromagnetic superconductor $EuFe_2(As_{0.7}P_{0.3})_2$, which shows a much lower coersive field (20 Oe at 2 K) [1] and a much higher saturation field (~7 kOe)[10].

Figure 5 plots the magnetic susceptibility M/H (left axis) and its reciprocal (right axis) of $RbEuFe_4As_4$ as functions of temperature. The M/H data exhibit a linear dependence in the high-T region, indicating dominant Curie-Weiss paramagnetism. We thus fit the data from 50 to 300 K by an extended Curie's law, $\chi = \chi_0 + C/(T - \theta)$, which yields $\chi_0 = 0.00178$ emu mol^{-1}, $C = 7.91$ emu K mol^{-1}, and $\theta = 23.6$ K. If one assumes that χ_0 is mostly contributed from Pauli paramagnetism, a density of state at Fermi level [$N(E_F)$] can be estimated to be 55 eV^{-1} fu^{-1}, which is unusually large. From the Curie constant C, an effective local moment of $\mu_{eff} = 7.95\mu_B$ fu^{-1} (fu denotes formula unit) is obtained, which is almost equal to the expected value of $g\sqrt{S(S+1)} = 7.94$ (μ_B) for an Eu^{2+} spin. The paramagnetic Curie temperature θ is positive, indicating dominant ferromagnetic interactions among the Eu spins. Indeed, in the low-T data shown in the inset of Fig. 5, a

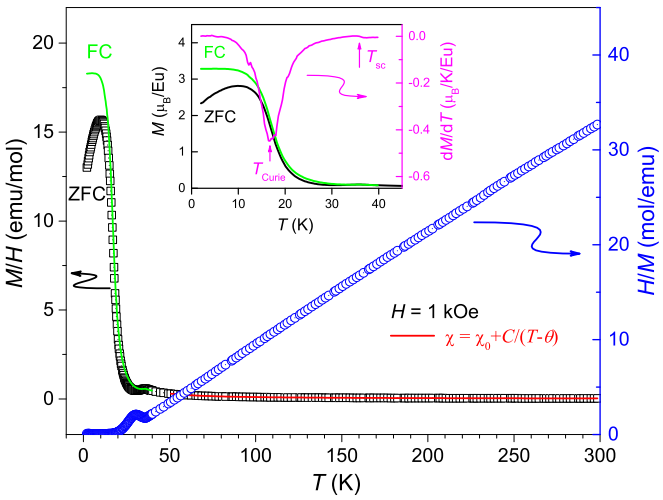

FIG. 5. Magnetic susceptibility (M/H) of $RbEuFe_4As_4$ measured under $H = 1$ kOe. The data from 50 to 300 K are fitted by the extended Curie law. The reciprocal of susceptibility (H/M) is shown using the right axis. The inset shows the temperature dependence of the magnetization in the low-T region, in which a canonical ferromagnetic transition can be seen. The T_{Curie} value can be estimated from the derivative of the magnetization (right axis).

canonical ferromagnetic transition can be seen. The transition temperature can be estimated by the dip in dM/dT [12], which is about 2 K higher than the T_{Curie} value at $H = 10$ Oe.

D. Specific heat

To further characterize the superconducting and magnetic transitions, we conducted heat capacity measurements for $RbEuFe_4As_4$. From the raw $C(T)$ data shown in Fig. 6(a), two anomalies at $T_{Curie} = 15$ K and $T_{sc} = 36.5$ K can be identified, respectively, verifying the ferromagnetic and superconducting transitions demonstrated above. The inset shows the superconducting transition more clearly. The thermodynamic transition temperature, determined by entropy-conserving construction, is 36.0 K, coincident with the zero-resistance temperature. Impressively, the specific-heat jump ΔC is as high as 7.5 J K^{-1} mol^{-1}, which further confirms bulk SC in $RbEuFe_4As_4$. The $\Delta C/T_{sc}$ value achieves 208 mJ K^{-2} mol^{-1}. Thus the electronic specific-heat coefficient γ can be estimated to be 145 mJ K^{-2} mol^{-1} by assuming $\Delta C/(\gamma T_{sc}) = 1.43$ in the BCS weak-coupling scenario. A similarly large γ value of ~150 mJ K^{-2} mol^{-1} can be *independently* estimated by the enhanced room-temperature specific heat, which is 46 J K^{-1} mol^{-1} larger than the Dulong-Petit limit $3NR$ ($N = 10$, being the number of atoms in a formula unit). Therefore the real γ value should be around 150 mJ K^{-2} mol^{-1}, equivalent to 38 mJ K^{-2} mol-Fe^{-1}. Such an enhanced γ is often observed in hole-doped FeSCs [41]. Notably, the estimated γ value corresponds to $N(E_F) \approx 60$ eV^{-1} fu^{-1}, consistent with the value derived from the magnetic measurement. Namely, the Wilson ratio is about unity albeit of an enhanced $N(E_F)$.

Figure 6(b) shows the variations in $C(T)$ under a magnetic field of 8 T. First, the superconducting transition temperature decreases slightly to 35.4 K, consistent with the result of the magneto-resistivity measurement above. Second, the anomaly at T_{Curie} is smeared out by the field. In addition, a minor anomaly at $T^* \sim 5$ K, which can be seen more easily in Figs. 6(c) and 6(d), tends to disappear as well. Third, the external field induces a $C(T)$-weight transfer from lower to higher temperatures. At $T < 20$ K, $C(T)$ is suppressed by the field; while in the temperature range of 22 K $< T <$ 100 K, $C(T)$ is enhanced substantially. The field-induced change in $C(T)$ has to be ascribed to the Eu-spin magnetism, because electronic and phonon specific heat (C_{el} and C_L) generally do not change with magnetic fields. The external fields force the Eu spins along the field direction, which severely broadens the phase transition, making the $C(T)$ weight shifts to higher temperatures consequently. Similar effect is also observed in $EuFe_2(As_{0.7}P_{0.3})_2$ [1].

The $C(T)$-weight transfer under different magnetic fields is explicitly shown in the C/T plot shown in Fig. 6(c). Besides, an upward shift of T_{Curie} can also be seen, further supporting the ferromagnetic transition. At $T^* \sim 5$ K, the zero-field C/T curve exhibits a tiny jump, which also changes with magnetic fields. Under a high field, the jump turns into a shoulder that moves to higher temperatures with increasing field. This sensitive response to magnetic fields suggests that it should be an intrinsic phenomenon. We will return to this topic in the Discussion section.

Shown in the inset of Fig. 6(c) is the C/T versus T^2 plot for the low-T data. As is known, the expected C/T value at $T \to 0$ K is zero for a fully gapped superconductor, which increases linearly with magnetic fields. However, the situation here is apparently abnormal: the zero-field C/T value is as large as 573 mJ K^{-2} mol^{-1} at 2 K, which is then suppressed to 86 mJ K^{-2} mol^{-1} at 8 T. This result suggests that the Eu-spin magnetic contribution (C_{Eu}) remains dominant around 2 K. Future measurements down to lower temperatures are expected to reveal the Eu-spin wave excitations as well as the quasiparticle excitations from the superconducting state.

Intriguingly, the specific-heat anomaly at T_{Curie} is very different from those of most magnetic orderings (such as those in $EuFe_2As_2$ [5] and $EuFe_2(As_{0.7}P_{0.3})_2$ [1]), which show a clear jump because of a second-order transition. In the present case for $RbEuFe_4As_4$, however, it simply shows a kink instead. We thus plot the derivative of specific heat, as shown in Fig. 6(d). An obvious jump at T_{Curie} can be seen in the zero-field dC/dT data. The result suggests that the magnetic transition is of a rare third-order type, according to the Ehrenfest classification [42]. To the best of our knowledge, no third-order magnetic transition has been reported in a real material before. As we know, most magnetic ordering transitions are described by Landau's second-order phase transition theory. Therefore, the observation of third-order magnetic transition deserves further investigations.

E. Discussion

$RbFe_2As_2$ is known to be a 2.6 K superconductor [43], while $EuFe_2As_2$ belongs to a parent compound of FeSCs [5]. Here we show that, interestingly, their hybrid material $RbEuFe_4As_4$ turns out to be a ferromagnetic superconductor. Similar material hybridization effect in FeSCs is witnessed in $Ba_2Ti_2Fe_2As_4O$ [44], which is actually an intergrowth of nonsuperconducting $BaTi_2As_2O$ and $BaFe_2As_2$.

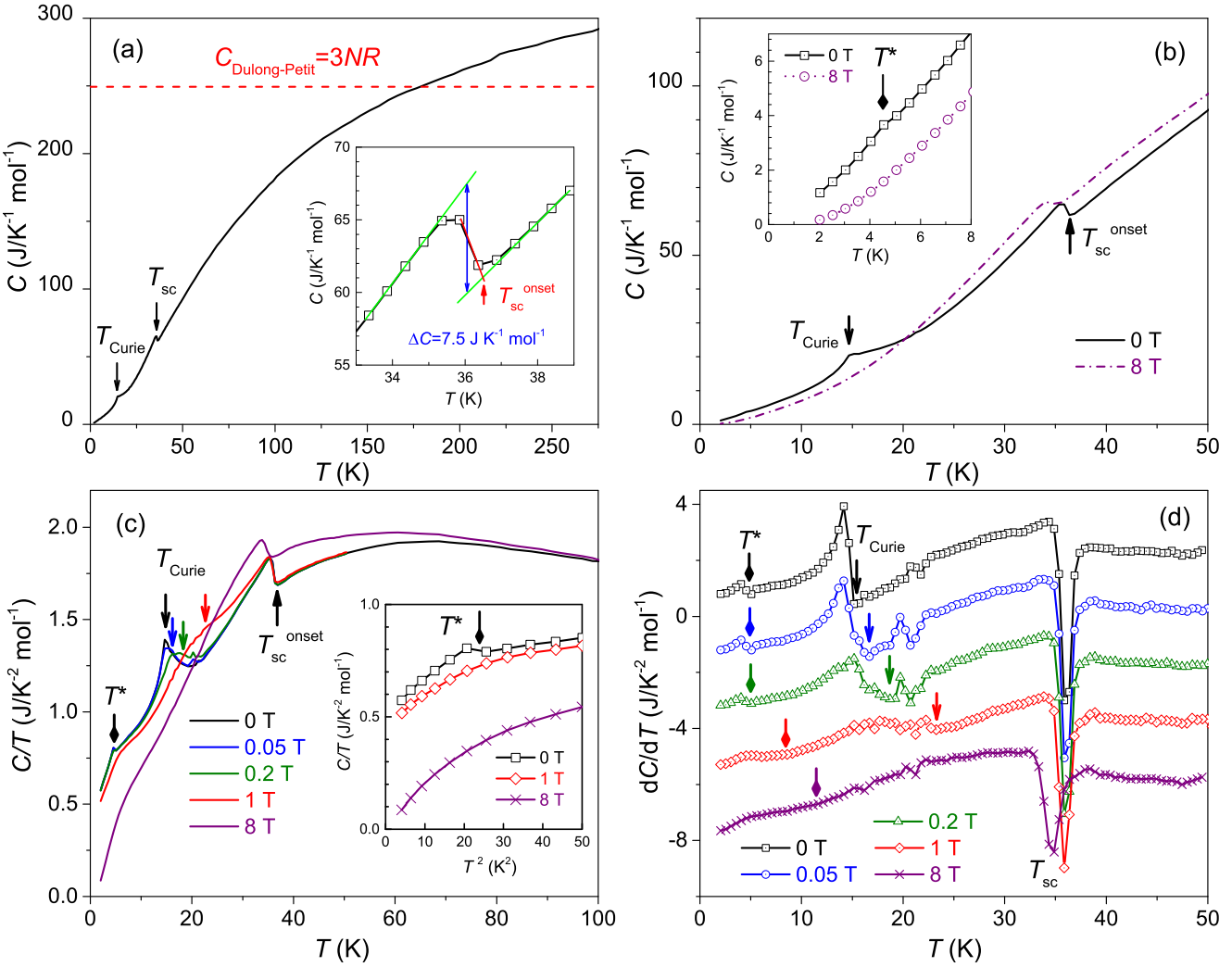

FIG. 6. Heat capacity measurements for $RbEuFe_4As_4$. The characteristic temperatures of superconducting transition (T_{sc}), ferromagnetic transition (T_{Curie}), and an unknown possible transition (T^*) are indicated by arrows, respectively. (a) Raw data of the specific heat, $C(T)$, at zero field. The inset zooms in the superconducting transition where a large specific-heat jump is determined. Panel (b) compares the $C(T)$ data at zero field and at 8 T. The inset magnifies the plot below 8 K, from which an anomaly can be distinguished at zero field. Panel(c) plots C/T vs T under various magnetic fields. The inserted plot shows C/T vs T^2 for the low-T data. (d) shows the derivative of specific heat (the data under fields are shifted downward for clarity).

$Ba_2Ti_2Fe_2As_4O$ shows SC at 21 K owing to a charge transfer between different layers, in relation with an electron-correlation effect [45]. Here in $RbEuFe_4As_4$, the isolated "$RbFe_2As_2$" block is heavily hole doped, in contrast with the undoped state in the "$EuFe_2As_2$" block. Consequently, the structural hybridization leads to a charge homogenization, since there is only one equivalent Fe site. Namely, $RbEuFe_4As_4$ is naturally hole doped by 25%. We hope that such a structural hybridization approach by design [32] may be utilized for future material explorations.

Notably, the T_{sc} value of $RbEuFe_4As_4$ is unexpectedly high, which is nearly equal to the maximum T_{sc} of 36.8 K for $CsSrFe_4As_4$ in the $AkAeFe_4As_4$ series [33]. Previous studies on doped $EuFe_2As_2$ superconductors show that the T_{sc} is always significantly lower than the Eu-free counterparts, which is ascribed to the Eu4f–Fe3d interaction. Therefore the unsuppressed T_{sc} in $RbEuFe_4As_4$ suggests vanishingly small Eu4f–Fe3$d_{yz/zx}$ coupling. The elongation of Eu − Fe interatomic distance from 3.604 Å in $EuFe_2As_2$ to 3.685 Å in $RbEuFe_4As_4$ supports this point of view. In addition, the high value of $\mu_0 dH_{c2}/dT|_{T_{sc}}$ (−5.6 T/K) as well as the large specific-heat jump (7.5 J K^{-1} mol^{-1}) further indicates robustness of SC in $RbEuFe_4As_4$.

In addition to the robust SC, evidence of Eu FM is also strong and sufficient. The $M(H)$ data show an obvious magnetic hysteresis (with a coersive field of 360 Oe at 2 K) as well as a saturation magnetization (6.5μ_B/Eu) that corresponds to Eu^{2+}-spin ferromagnetic alignment. Besides, both the positive paramagnetic Curie temperature and the increase of T_{Curie} with magnetic field support the ferromagnetic transition scenario. Hopefully, future measurements of the anisotropic magnetic properties using single crystal samples will give more information on the magnetic state. Needless to say, investigations of the Mössbauer spectra, x-ray resonant

magnetic scattering and neutron scattering will be definitely helpful to clarity the Eu-spin orientation and other related information.

The appearance of Eu FM in $RbEuFe_4As_4$ can be explained in terms of modification of $J_R^{\perp}$, since $J_R^{\perp}$ [$\propto \cos(2k_F r)/r^3$] *oscillates* and tends to decay with $r_{\perp}$. In $RbEuFe_4As_4$, the interlayer Eu interatomic distance $r_{\perp}$ becomes 13.31 Å, which is almost twice as the $r_{\perp}$ value in $EuFe_2As_2$ (6.657 Å). This may change the sign of $J_R^{\perp}$, resulting in an Eu FM. The lowered Curie temperature [about 4 K lower than that of $EuFe_2(As_{0.7}P_{0.3})_2$] seems to be associated with the decay of $J_R^{\perp}$. The weak interlayer magnetic coupling not only accounts for the relatively low Curie temperature, but also justifies the robustness of SC. Additionally, it could be related to the third-order transition observed, because of the enhanced two dimensionality which allows strong magnetic fluctuations above T_{Curie}.

Finally, let us discuss how SC and FM compromise in $RbEuFe_4As_4$. There were a few theoretical proposals available on the FM+SC issue decades ago [46–50]. The first solution is that FM is modified in the form of a "cryptoferromagnetic" state or a multidomain structure (with domain size d), hence the superconducting Cooper pairs feel no net magnetization if the superconducting coherent length satisfies $\xi \gg d$ [46]. The second idea considers that superconducting Cooper pairs are "magnetized" by the exchange fields, such that they possess nonzero momentum [47], or equivalently, SC is modulated to be inhomogeneous in real space [48]. This scenario is often called Fulde-Ferrell-Larkin-Ovchinnikov (FFLO) state. Alternatively, the internal spontaneous magnetization field from FM penetrates the superconductor, which induces "spontaneous vortices" even at zero external field, hence called spontaneous vortex (SV) state [49,50]. Since nonsuperconducting defects tend to trap spontaneous vortices, the FFLO state is believed to be possible only in a clean-limit superconductor. As for the $RbEuFe_4As_4$ system, the first candidate seems to be unlikely, because the estimated coherence length at zero temperature is only 1.52 nm [51], which constrains the ferromagnetic domain size too much to present a long-range order. Note that the residual resistivity tends to be very small by a rough extrapolation (see Fig. 2) even for the polycrystalline sample, which means a quite long electron mean free path and, the flux-pinning effect is not severe from the FC diamagnetic signal (see Fig. 3). These facts suggest that the superconductor is probably in a clean limit at lower temperatures. We thus speculate that the anomaly at $T^* \sim 5$ K could be related to the change in the way of FM+SC. There are indeed some signatures. The bifurcation of FCC and FCH curves above T^*, shown in Fig. 3, implies the transformation from FFLO to SV state. The small specific-heat jump at T^* [Fig. 6(c)] suggests a weak phase transition. In addition, T^* increases with field. Obviously, more investigations are needed to address this interesting issue.

IV. CONCLUSION

To summarize, we have discovered an iron-based compound $RbEuFe_4As_4$ in which an unprecedented coexistence of SC and FM is observed. The new material crystallizes in an intergrowth structure of body-centered $RbFe_2As_2$ and $EuFe_2As_2$, which drastically changes the physical properties. The FeAs layers are found to be hole doped by the material itself, presenting a large normal-state electronic specific-heat coefficient (~150 mJ K^{-2} mol^{-1}) and a Pauli spin susceptibility (~0.00178 emu mol^{-1}). Bulk superconductivity at $T_{sc} = 36.5$ K and Eu-spin ferromagnetism at 15 K are unambiguously demonstrated. The specific-heat jump at T_{sc} is as high as 7.5 J K^{-1} mol^{-1}. The Eu-spin ferromagnetism is manifested by a magnetic hysteresis with a 360-Oe coersive field at 2 K, a saturation magnetization of $6.5\mu_B$/Eu, and a saturation field of ~1.5 kOe at low temperatures.

There are two additional novel phenomena observed in $RbEuFe_4As_4$. First, the Eu-spin ferromagnetic transition is of a rare third order, evidenced by the continuity in $C(T)$ and discontinuity in dC/dT at T_{Curie}. Second, a weak anomaly at about 5 K possibly reflects the interplay between SC and FM. These intriguing observations together with the robust coexistence of SC and FM call for further investigations on the interesting title material.

ACKNOWLEDGMENTS

This work was supported by the National Science Foundation of China (under Grants No. 11474252, No. 90922002, and No. 11190023) and the Fundamental Research Funds for the Central Universities of China.

[1] Z. Ren, Q. Tao, S. Jiang, C. Feng, C. Wang, J. Dai, G. Cao, and Z. Xu, Superconductivity Induced by Phosphorus Doping and Its Coexistence with Ferromagnetism in $EuFe_2(As_{0.7}P_{0.3})_2$, Phys. Rev. Lett. **102**, 137002 (2009).

[2] I. Nowik, I. Felner, Z. Ren, G. H. Cao, and Z. A. Xu, Coexistence of ferromagnetism and superconductivity: Magnetization and Mössbauer studies of $EuFe_2(As_{1-x}P_x)_2$, J. Phys.: Condens. Matt. **23**, 065701 (2011).

[3] S. Nandi, W. T. Jin, Y. Xiao, Y. Su, S. Price, D. K. Shukla, J. Strempfer, H. S. Jeevan, P. Gegenwart, and T. Brückel, Coexistence of superconductivity and ferromagnetism in P-doped $EuFe_2As_2$, Phys. Rev. B **89**, 014512 (2014).

[4] S. Nandi, W. T. Jin, Y. Xiao, Y. Su, S. Price, W. Schmidt, K. Schmalzl, T. Chatterji, H. S. Jeevan, P. Gegenwart, and T. Brückel, Magnetic structure of the Eu^{2+} moments in superconducting $EuFe_2(As_{1-x}P_x)_2$ with $x = 0.19$, Phys. Rev. B **90**, 094407 (2014).

[5] Z. Ren, Z. Zhu, S. Jiang, X. Xu, Q. Tao, C. Wang, C. Feng, G. Cao, and Z. Xu, Antiferromagnetic transition in $EuFe_2As_2$: A possible parent compound for superconductors, Phys. Rev. B **78**, 052501 (2008).

[6] H. S. Jeevan, Z. Hossain, D. Kasinathan, H. Rosner, C. Geibel, and P. Gegenwart, Electrical resistivity and specific heat of single-crystalline $EuFe_2As_2$: A

magnetic homologue of $SrFe_2As_2$, Phys. Rev. B **78**, 052502 (2008).

[7] S. Jiang, Y. Luo, Z. Ren, Z. Zhu, C. Wang, X. Xu, Q. Tao, G. Cao, and Z. Xu, Metamagnetic transition in $EuFe_2As_2$ single crystals, New J. Phys. **11**, 025007 (2009).

[8] J. Herrero-Martín, V. Scagnoli, C. Mazzoli, Y. Su, R. Mittal, Y. Xiao, T. Brueckel, N. Kumar, S. K. Dhar, A. Thamizhavel, and L. Paolasini, Magnetic structure of $EuFe_2As_2$ as determined by resonant x-ray scattering, Phys. Rev. B **80**, 134411 (2009).

[9] Y. Xiao, Y. Su, M. Meven, R. Mittal, C. M. N. Kumar, T. Chatterji, S. Price, J. Persson, N. Kumar, S. K. Dhar, A. Thamizhavel, and T. Brueckel, Magnetic structure of $EuFe_2As_2$ determined by single-crystal neutron diffraction, Phys. Rev. B **80**, 174424 (2009).

[10] G. Cao, S. Xu, Z. Ren, S. Jiang, C. Feng, and Z. Xu, Superconductivity and ferromagnetism in $EuFe_2(As_{1-x}P_x)_2$, J. Phys.: Condens. Matt. **23**, 464204 (2011).

[11] H. S. Jeevan, D. Kasinathan, H. Rosner, and P. Gegenwart, Interplay of antiferromagnetism, ferromagnetism, and superconductivity in $EuFe_2(As_{1-x}P_x)_2$ single crystals, Phys. Rev. B **83**, 054511 (2011).

[12] S. Jiang, H. Xing, G. Xuan, Z. Ren, C. Wang, Z.-a. Xu, and G. Cao, Superconductivity and local-moment magnetism in $Eu(Fe_{0.89}Co_{0.11})_2As_2$, Phys. Rev. B **80**, 184514 (2009).

[13] W.-H. Jiao, Q. Tao, J.-K. Bao, Y.-L. Sun, C.-M. Feng, Z.-A. Xu, I. Nowik, I. Felner, and G.-H. Cao, Anisotropic superconductivity in $Eu(Fe_{0.75}Ru_{0.25})_2As_2$ ferromagnetic superconductor, Europhys. Lett. **95**, 67007 (2011).

[14] W.-H. Jiao, H.-F. Zhai, J.-K. Bao, Y.-K. Luo, Q. Tao, C.-M. Feng, Z.-A. Xu, and G.-H. Cao, Anomalous critical fields and the absence of Meissner state in $Eu(Fe_{0.88}Ir_{0.12})_2As_2$ crystals, New J. Phys. **15**, 113002 (2013).

[15] W. T. Jin, S. Nandi, Y. Xiao, Y. Su, O. Zaharko, Z. Guguchia, Z. Bukowski, S. Price, W. H. Jiao, G. H. Cao, and T. Brückel, Magnetic structure of superconducting $Eu(Fe_{0.82}Co_{0.18})_2As_2$ as revealed by single-crystal neutron diffraction, Phys. Rev. B **88**, 214516 (2013).

[16] W. T. Jin, W. Li, Y. Su, S. Nandi, Y. Xiao, W. H. Jiao, M. Meven, A. P. Sazonov, E. Feng, Y. Chen, C. S. Ting, G. H. Cao, and T. Brückel, Magnetic ground state of superconducting $Eu(Fe_{0.88}Ir_{0.12})_2As_2$: A combined neutron diffraction and first-principles calculation study, Phys. Rev. B **91**, 064506 (2015).

[17] Y. Tokiwa, S.-H. Hübner, O. Beck, H. S. Jeevan, and P. Gegenwart, Unique phase diagram with narrow superconducting dome in $EuFe_2(As_{1-x}P_x)_2$ due to Eu^{2+} local magnetic moments, Phys. Rev. B **86**, 220505 (2012).

[18] S. Zapf, D. Wu, L. Bogani, H. S. Jeevan, P. Gegenwart, and M. Dressel, Varying Eu^{2+} magnetic order by chemical pressure in $EuFe_2(As_{1-x}P_x)_2$, Phys. Rev. B **84**, 140503 (2011).

[19] S. Zapf, H. S. Jeevan, T. Ivek, F. Pfister, F. Klingert, S. Jiang, D. Wu, P. Gegenwart, R. K. Kremer, and M. Dressel, $EuFe_2(As_{1-x}P_x)_2$: Reentrant Spin Glass and Superconductivity, Phys. Rev. Lett. **110**, 237002 (2013).

[20] A. Błachowski, K. Ruebenbauer, J. Żukrowski, Z. Bukowski, K. Rogacki, P. J. W. Moll, and J. Karpinski, Interplay between magnetism and superconductivity in $EuFe_{2-x}Co_xAs_2$ studied by ^{57}Fe and ^{151}Eu Mössbauer spectroscopy, Phys. Rev. B **84**, 174503 (2011).

[21] V. L. Ginzburg, Ferromagnetic superconductors, Sov. Phys. JETP-USSR **4**, 153 (1957).

[22] L. N. Bulaevskii, A. I. Buzdin, M. L. Kulic, and S. V. Panjukov, Coexistence of superconductivity and magnetism - theoretical predictions and experimental results, Adv. Phys. **34**, 175 (1985).

[23] C. Wolowiec, B. White, and M. Maple, Conventional magnetic superconductors, Physica C **514**, 113 (2015).

[24] Note that spin-triplet superconductivity may coexist with itinerant ferromagnetism in some U-containing materials. The related information can be seen in a recent review article [A. D. Huxley, Ferromagnetic superconductors, Physica C **514**, 368 (2015)].

[25] G.-H. Cao, W.-H. Jiao, Y.-K. Luo, Z. Ren, S. Jiang, and Z.-A. Xu, Coexistence of superconductivity and ferromagnetism in iron pnictides, J. Phys.: Conf. Ser. **391**, 012123 (2012).

[26] D. C. Johnston, The puzzle of high-temperature superconductivity in layered iron pnictides and chalcogenides, Adv. Phys. **59**, 803 (2010).

[27] G. R. Stewart, Superconductivity in iron compounds, Rev. Mod. Phys. **83**, 1589 (2011).

[28] S. Raghu, X.-L. Qi, C.-X. Liu, D. J. Scalapino, and S.-C. Zhang, Minimal two-band model of the superconducting iron oxypnictides, Phys. Rev. B **77**, 220503 (2008).

[29] Z. Ren, X. Lin, Q. Tao, S. Jiang, Z. Zhu, C. Wang, G. Cao, and Z. Xu, Suppression of spin-density-wave transition and emergence of ferromagnetic ordering of Eu^{2+} moments in $EuFe_{2-x}Ni_xAs_2$, Phys. Rev. B **79**, 094426 (2009).

[30] D. J. Singh and M.-H. Du, Density Functional Study of $LaFeAsO_{1-x}F_x$: A Low Carrier Density Superconductor Near Itinerant Magnetism, Phys. Rev. Lett. **100**, 237003 (2008).

[31] W. Li, J.-X. Zhu, Y. Chen, and C. S. Ting, First-principles calculations of the electronic structure of iron-pnictide $EuFe_2(As,P)_2$ superconductors: Evidence for antiferromagnetic spin order, Phys. Rev. B **86**, 155119 (2012).

[32] H. Jiang, Y.-L. Sun, Z.-A. Xu, and G.-H. Cao, Crystal chemistry and structural design of iron-based superconductors, Chin. Phys. B **22**, 087410 (2013).

[33] A. Iyo, K. Kawashima, T. Kinjo, T. Nishio, S. Ishida, H. Fujihisa, Y. Gotoh, K. Kihou, H. Eisaki, and Y. Yoshida, New-structure-type fe-based superconductors: $CaAFe_4As_4$ (A = K, Rb, Cs) and $SrAFe_4As_4$ (A = Rb, Cs), J. Am. Chem. Soc. **138**, 3410 (2016).

[34] F. Izumi and K. Momma, Three-dimensional visualization in powder diffraction, in *Applied Crystallography XX*, edited by D. Stroz and M. Karolus, Solid State Phenomena Vol. 130 (Elsevier, North Holland, 2007), pp. 15–20.

[35] H. H. Sample, W. J. Bruno, S. B. Sample, and E. K. Sichel, Reverse-field reciprocity for conducting specimens in magnetic fields, J. Appl. Phys. **61**, 1079 (1987).

[36] P. Wenz and H. U. Schuster, New ternary intermetallic phases of potasium and rubidium with 8B-elements and 5B-elements, Z. Nat. Sect. B **39**, 1816 (1984).

[37] M. Rotter, M. Tegel, and D. Johrendt, Superconductivity at 38 K in the Iron Arsenide $(Ba_{1-x}K_x)Fe_2As_2$, Phys. Rev. Lett. **101**, 107006 (2008).

[38] B. Shen, H. Yang, Z.-S. Wang, F. Han, B. Zeng, L. Shan, C. Ren, and H.-H. Wen, Transport properties and asymmetric scattering in $Ba_{1-x}K_xFe_2As_2$ single crystals, Phys. Rev. B **84**, 184512 (2011).

[39] H. S. Jeevan, Z. Hossain, D. Kasinathan, H. Rosner, C. Geibel, and P. Gegenwart, High-temperature superconductivity in $Eu_{0.5}K_{0.5}Fe_2As_2$, Phys. Rev. B **78**, 092406 (2008).

[40] W. A. Fertig, D. C. Johnston, L. E. DeLong, R. W. McCallum, M. B. Maple, and B. T. Matthias, Destruction of Superconductivity at the Onset of Long-Range Magnetic Order in the Compound $ErRh_4B_4$, Phys. Rev. Lett. **38**, 987 (1977).

[41] G. Mu, H. Luo, Z. Wang, L. Shan, C. Ren, and H.-H. Wen, Low temperature specific heat of the hole-doped $Ba_{0.6}K_{0.4}Fe_2As_2$ single crystals, Phys. Rev. B **79**, 174501 (2009).

[42] G. Jaeger, The Ehrenfest classification of phase transitions: Introduction and evolution, Arch. Hist. Exact Sci. **53**, 51 (1998).

[43] Z. Bukowski, S. Weyeneth, R. Puzniak, J. Karpinski, and B. Batlogg, Bulk superconductivity at 2.6 K in undoped $RbFe_2As_2$, Physica C **470** (Suppl. 1), S328 (2010).

[44] Y.-L. Sun, H. Jiang, H.-F. Zhai, J.-K. Bao, W.-H. Jiao, Q. Tao, C.-Y. Shen, Y.-W. Zeng, Z.-A. Xu, and G.-H. Cao, $Ba_2Ti_2Fe_2As_4O$: A new superconductor containing Fe_2As_2 layers and Ti_2O sheets, J. Am. Chem. Soc. **134**, 12893 (2012).

[45] J.-Z. Ma, A. van Roekeghem, P. Richard, Z.-H. Liu, H. Miao, L.-K. Zeng, N. Xu, M. Shi, C. Cao, J.-B. He, G.-F. Chen, Y.-L. Sun, G.-H. Cao, S.-C. Wang, S. Biermann, T. Qian, and H. Ding, Correlation-Induced Self-Doping in the Iron-Pnictide Superconductor $Ba_2Ti_2Fe_2As_4O$, Phys. Rev. Lett. **113**, 266407 (2014).

[46] P. W. Anderson and H. Suhl, Spin Alignment in the Superconducting State, Phys. Rev. **116**, 898 (1959).

[47] P. Fulde and R. A. Ferrell, Superconductivity in a strong spin-exchange field, Phys. Rev. **135**, A550 (1964).

[48] A. I. Larkin and Ovchinni.Yn, Inhomogeneous state of superconductors, Sov. Phys. JETP-USSR **20**, 762 (1965).

[49] H. S. Greenside, E. I. Blount, and C. M. Varma, Possible Coexisting Superconducting and Magnetic States, Phys. Rev. Lett. **46**, 49 (1981).

[50] M. Tachiki, H. Matsumoto, T. Koyama, and H. Umezawa, Self-induced vortices in magnetic superconductors, Solid State Commun. **34**, 19 (1980).

[51] The coherence length is calculated by $\xi(0) = \phi_0/[2\pi H_{c2}^{orb}(0)]$, where $H_{c2}^{orb}(0)$ is obtained by the slope of $H_{c2}(T)$ (-5.6 T/K) using the Werthamer-Helfand-Hohenberg formula $H_{c2}^{orb}(0) = -0.693 T_{sc}(\mu_0 d H_{c2}/dT|_{T_{sc}}) = 141.6$ T.